SCIENTIFIC REPORTS

OPEN

SUBJECT AREAS:
SPINTRONICS
MAGNETIC PROPERTIES AND MATERIALS

Received
8 April 2014

Accepted
24 July 2014

Published
1 October 2014

Correspondence and requests for materials should be addressed to L.V. (laurent.vila@cea.fr) or J.P.A. (jean-philippe.attane@cea.fr)

# Elementary depinning processes of magnetic domain walls under fields and currents

V. D. Nguyen[1,2], W. Savero Torres[1], P. Laczkowski[1], A. Marty[1], M. Jamet[1], C. Beigné[1], L. Notin[1], L. Vila[1] & J. P. Attané[1]

[1]INAC/CEA Grenoble and Université Joseph Fourier, 38054, Grenoble, France, [2]Institut Néel and Université Joseph Fourier, 38042 Grenoble, France.

**The probability laws associated to domain wall depinning under fields and currents have been studied in NiFe and FePt nanowires. Three basic domain wall depinning processes, associated to different potential landscapes, are found to appear identically in those systems with very different anisotropies. We show that these processes constitute the building blocks of any complex depinning mechanism. A Markovian analysis is proposed, that provides a unified picture of the depinning mechanism and an insight into the pinning potential landscape.**

The precise control of domain wall (DW) pinning and depinning in nanowires is crucial for the operation of new spintronics devices based on DW motion. However, the engineering of appropriate pinning sites is difficult to achieve: depinning mechanisms are not clearly understood yet, especially since the pinning potential seen by the DW can be very complex. This complexity appears in particular through the stochastic behaviour of DW depinning, which has been experimentally observed in systems with perpendicular[1–6] and planar magnetization[7–14]. This stochasticity has been also investigated using simulations or analytical models. If it could become a major challenge for practical applications, even in the *nanosecond* range[6], it is also very sensitive to the application of currents, and thus provides a way to probe spin transfer effects at low current densities[2,18].

Two sources of randomness have been identified: the first one is the thermal activation[1], and the second one the ability for the DW to be randomly pinned on a given defect along different micromagnetic configurations. These sources are known to affect the statistical distribution of pinning times when constant fields or currents are applied[15], or the distribution of pinning fields in field sweeping experiments[14].

In the following, we study DW depinning under field and/or current, in nanowires with both perpendicular (FePt) and planar (NiFe) magnetization. Using different kind of constriction to pin the DW, we show that although the observed behaviour is often complex, we can provide a unified picture of stochastic depinning by identifying three elementary behaviours as the building blocks of any depinning mechanism.

FePt-based spin-valves [FePt(5 nm)/Pd(2 nm)/FePt(5 nm)//MgO] with high perpendicular anisotropy have been grown by molecular beam epitaxy[16]. 30 nm thick NiFe samples were deposited by e-beam evaporation. Nanowires have then been processed in both kinds of layers using e-beam lithography techniques (see Fig. 1a). The FePt and NiFe nanowires are respectively 200 nm and 100 nm wide, and constrictions are patterned in order to pin the DW.

The position of the DW along the wire is detected using transport techniques: a small AC current ($J = 2.10^9$ $A/m^2$, $f = 1023$ $Hz$ for FePt and $J = 3.10^{10}$ $A/m^2$, $f = 6700$ $Hz$ for NiFe) is injected in the main wire, while a lock-in registers the voltage between two transverse contacts. A field close to the depinning field of the DW is applied, either perpendicularly to the layer (FePt) or along the main wire direction (NiFe). For NiFe devices, the DW position is then detected using a combination of Anisotropic Magneto-Resistance (AMR) and Magnon Magneto-Resistance (MMR)[17] (cf. fig. 1b). For FePt devices, the spin-valve structure allows using the Giant Magneto-Resistance (GMR) effect (cf. fig. 1d). The observed signals indicate that a DW is injected from the nucleation pad, gets quickly pinned on the constriction where it stays for a while. Then a depinning event occurs, followed by DW propagation.

As the pinning time is found to be stochastic, the measurement has to be repeated several times (usually 400) in order to determine its associated probability law. Such probability laws can be represented using the cumulative distribution functions of the pinning time P(t), *i.e.*, the probability to be depinned at time t. Several series of measurements have been realized using different geometries of the constriction. The data analysis shows that in

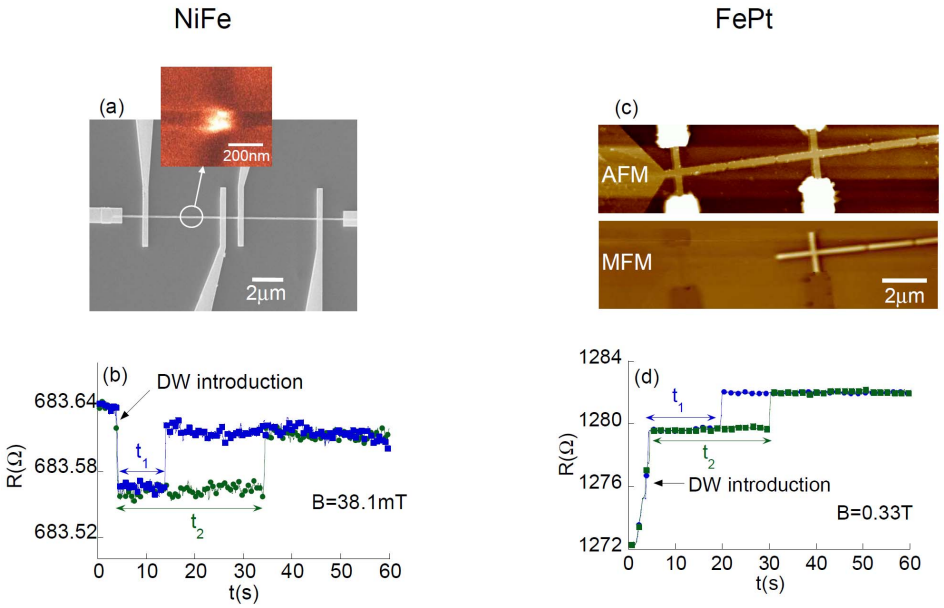


**Figure 1** | (a) SEM image of a 100 nm wide NiFe nanowire with Au pads for electrical contacts, and MFM image (inset) showing a DW pinned on the 50 nm wide constriction. (b) The DW motion is detected using a resistance measurement, probing both the AMR and the MMR, and a constant field is applied to the sample. A DW is introduced in the constriction, where it gets pinned for a while. The pinning time is stochastic, varying from experiment to experiment. Here are shown two examples of measurements realized using the same experimental conditions, but leading to different pinning times $t_1$ and $t_2$. (c) AFM and MFM images of a 200 nm wide FePt/Pd/FePt nanowire. The MFM image shows a single DW pinned on a 80 nm wide constriction. (d) Variation of the GMR as a function of time, associated to the motion of the DW between the two contacts. Here again, the two different pinning times obtained by repeating the measurement illustrate the stochastic behaviour of DW depinning.

both systems, three basic kinds of probability laws can be identified. Indeed, whereas P(t) curves of fig. 2a and 2b are regular exponential laws, in figs. 2d and 2e the initial depinning probability density vanishes, (i.e., $\left.\frac{\partial P}{\partial t}\right|_{t=0}=0$), and in figs. 2g and 2h the long time cumulative distribution stays below 1 ($\lim_{t\to\infty} P \neq 1$).

We will show in the following that these three curves correspond to the three elementary depinning behaviours: the DW depinning occurs along either a simple path, serial paths, or alternative paths.

As seen in figs. 2a and 2b, in the case of a simple path, the P(t) curves can be fitted by an exponential law

$$P(t)=1-\exp[-\frac{t}{\tau}] \quad (1)$$

Where τ, the mean pinning time, depends on the attempt frequency $f_0$ and on the energy barrier height E(B):

$$\frac{1}{\tau}=f_0\ \exp[-\frac{E(B)}{k_B T}] \quad (2)$$

This stochasticity corresponds to the random crossing of a single energy barrier due to thermal activation (cf. fig. 2c). This phenomenon has been already observed in a system with planar magnetization[9], and can be reproduced by micromagnetic simulations taking into account thermal activation[18,19]. In perpendicular systems, this behaviour has been observed in CoNi and CoPt with constrictions[2,4,5]. In FePt, however, the behaviour observed previously in FePt nanowires without constrictions was those of figs. 2 g,h[1,2,20]. The appearance of a simple exponential law when using the constriction of fig. 2a is probably due to the fact that the constriction constrains the DW, simplifying the energy landscape by reducing the number of available pinned configurations. Therefore, there remains only one configuration for the pinned state, and the depinning involves a single energy barrier.

In the range of studied fields, as shown later, the energy barrier is found to vary linearly accordingly to a simple 1D model[1,21]:

$$E(B)=E_0-2BVM_S \quad (3)$$

with $M_S$(FePt) = $1.03\times10^6$ A.m$^{-1}$, V being the magnetic volume reversed by the elementary depinning process (activation volume) and $E_0$ the energy barrier at zero field. In the case of a simple path (fig. 2a and 2b), eq. [3] can be used to extract the activations volumes and the energy barriers at room temperature: for FePt V = 266 nm$^3$ and $E_0$ = 1.44 eV, for NiFe V = 2613 nm$^3$ and $E_0$ = 1.7 eV.

In figs. 2d and 2e appears a yet unobserved behaviour, with a derivative of P(t) equal to zero at t = 0. This behaviour can be understood as a depinning process along serial paths: the energy landscape is such that the DW has to cross sequentially two barriers to get depinned, as illustrated in fig. 2f. In this figure, state 1 is the pinned state, state 2 is an intermediary pinned state, and state 3 the depinned state. In both states 1 and 2, the DW is in the constriction, but at different positions or with different micromagnetic configurations. It is possible to calculate P(t) assuming that the depinning process is a Markov homogeneous process: under the influence of the applied field and of the temperature, the system jump stochastically from one state *i* to an other state *j* with a frequency $1/\tau_{ij}$. Let us note

$$\vec{\Omega}(t)=[P_1(t),P_2(t),P_3(t)] \quad (4)$$

the vector whose $i^{th}$ component is the probability to be in the $i^{th}$ state at time t. For example the DW is always pinned in state 1 at t = 0, and thus the boundary condition can be written

$$\vec{\Omega}(0)=[1\quad 0\quad 0] \quad (5)$$

The Markov matrix corresponding to this sequential paths case is

$$M=\begin{pmatrix} -\frac{1}{\tau_{12}} & \frac{1}{\tau_{12}} & 0 \\ 0 & -\frac{1}{\tau_{23}} & \frac{1}{\tau_{23}} \\ 0 & 0 & 0 \end{pmatrix} \quad (6)$$

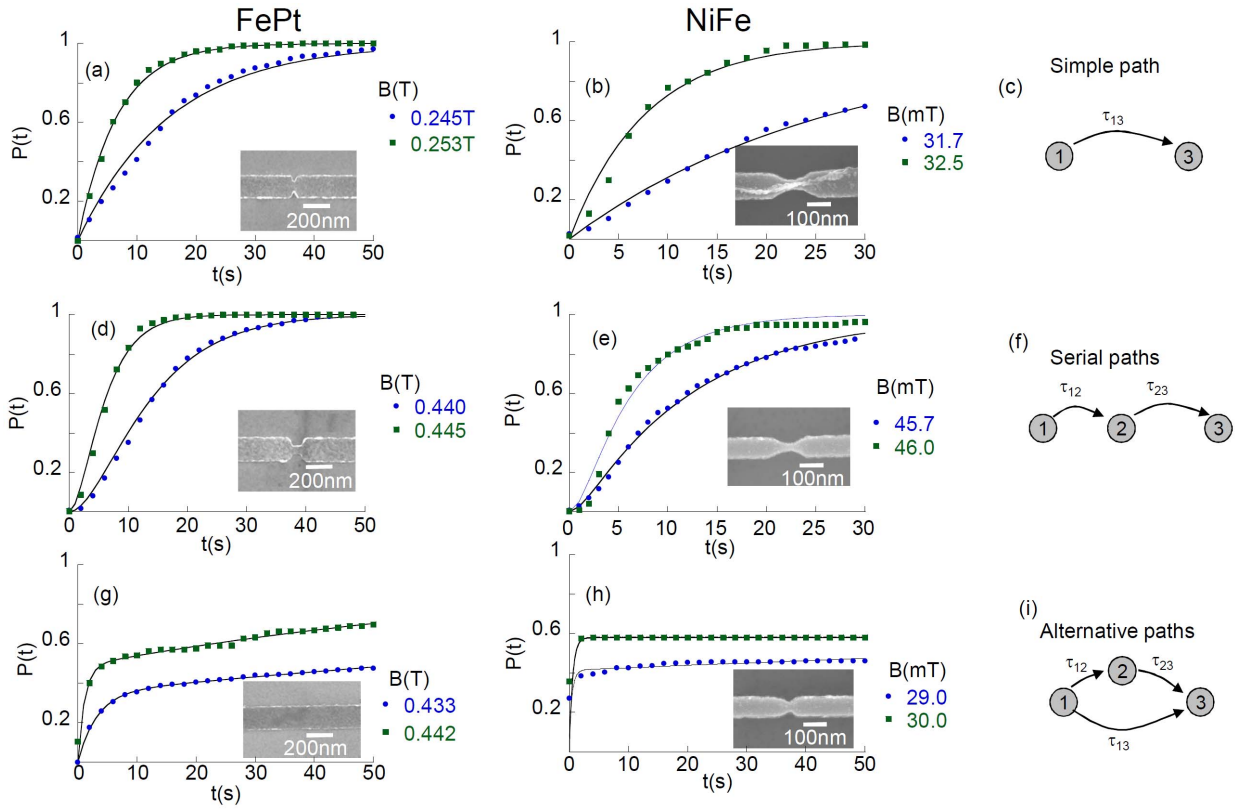


**Figure 2** | Cumulative probability functions P(t) of the pinning time, for different constant magnetic fields B. In both systems (FePt on the left, NiFe on the right), three behavior can be observed: simple (a,b), serial (d, e) and alternative paths for (g, h). The inset of each curve is a SEM image of the constriction shape. The points are experimental data, and the lines correspond to fits using the model proposed in this letter. Fig., (c, f, i) show the schematic illustration of the Markov process for the 3 different mechanism of DW depinning.

The evolution of the system is then given by the differential equation:

$$\frac{d\vec{\Omega}(t)}{dt} = \vec{\Omega}(t)M \tag{7}$$

which leads to

$$\mathrm{P(t)} = \vec{\Omega}(\mathrm{t}).\begin{bmatrix}0\\0\\1\end{bmatrix} = [1 \quad 0 \quad 0]\exp[\mathrm{tM}]\begin{bmatrix}0\\0\\1\end{bmatrix} \tag{8}$$

and finally to

$$\mathrm{P(t)} = \frac{\tau_{12}(1-e^{-\frac{t}{\tau_{12}}}) - \tau_{23}(1-e^{-\frac{t}{\tau_{23}}})}{\tau_{12}-\tau_{23}} \tag{9}$$

In this case, we retrieve $\left.\frac{\partial P}{\partial t}\right|_{t=0} = 0$, and our data can be fitted by this probability law. Also, in one FePt device we managed to observe more closely this phenomenon. The pinning on the constriction is evidenced by a plateau in the GMR signal. Low-noise measurements show that it is actually divided in two sub-plateaus, corresponding to two different positions or micromagnetic states of the pinned DW, *i.e.*, to the states 1 and 2 of our analysis (cf. fig. 3a). A statistical analysis shows that, in accordance to our model, state 1 always appears before state 2, and that the pinning times in state 1 only and in state 2 only both follow exponential laws, whereas the overall pinning time on the constriction follow the probability law of equation 9 (cf. fig. 3b).

The third depinning behaviour appears in figs. 2g and 2h, and corresponds to alternative paths. The DW begins in state 1, and in addition to a direct path $1 \rightarrow 3$ an alternative path $1 \rightarrow 2 \rightarrow 3$ can be taken (cf. fig. 2i). This assumes that the DW can change its configuration from 1 to 2 while remaining pinned, in a way similar to the thermally activated transitions from one wall type to another (transverse-vortex)[22], or to the vortex switching process[27]. It has been shown in planar systems that different kind of DW (chirality of the DW[23–25], or DW type[8,11,13,14,26,27] could lead to different depinning fields or depinning currents[28]. Here, if the DW is pinned in state 1, it can get depinned by thermal activation, which leads to the exponential-like behaviour of P(t). However, when pinned in state 2, it stays forever in state 2, which gives account of the non-saturation of P(t) (cf. field-sweeping experiments in Supplemental Material at [SM URL]).

This behaviour corresponds to the Markov process of fig. 2i, and to the Markov Matrix[1]:

$$\mathrm{M} = \begin{pmatrix} -\left(\frac{1}{\tau_{12}}+\frac{1}{\tau_{13}}\right) & \frac{1}{\tau_{12}} & \frac{1}{\tau_{13}} \\ 0 & -\frac{1}{\tau_{23}} & \frac{1}{\tau_{23}} \\ 0 & 0 & 0 \end{pmatrix} \tag{10}$$

leading to

$$\mathrm{P(t)} = 1-(1-r)e^{-t\left(\frac{1}{\tau_{12}}+\frac{1}{\tau_{13}}\right)} - re^{\frac{-t}{\tau_{23}}} \tag{11}$$

where $r = \frac{1/\tau_{12}}{1/\tau_{12}+1/\tau_{13}-1/\tau_{23}}$.

Note that the proposed Markov analysis can be extended to more complex cases: processes involving n micromagnetic states, cases where backward and forward jumps from state i to state j lead to telegraphic noise[3,10], and field-sweeping experiments (See

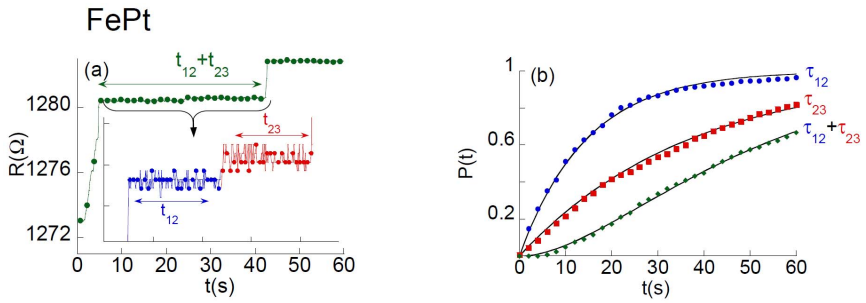


**Figure 3** | (a) Variation of GMR as a function of time showing two different steps of resistance which correspond to two different positions of the pinned DW. The inset is a zoom of the plateau of resistance. (b) Cumulative functions P(t) of the DW pinned on the two different positions (blue and red curves). The corresponding processes follow a single exponential law, with mean pinning time $\tau_{12}$ and $\tau_{23}$, respectively. The green curve corresponds to the total pinning process, and exhibits a zero derivative at $t = 0$.

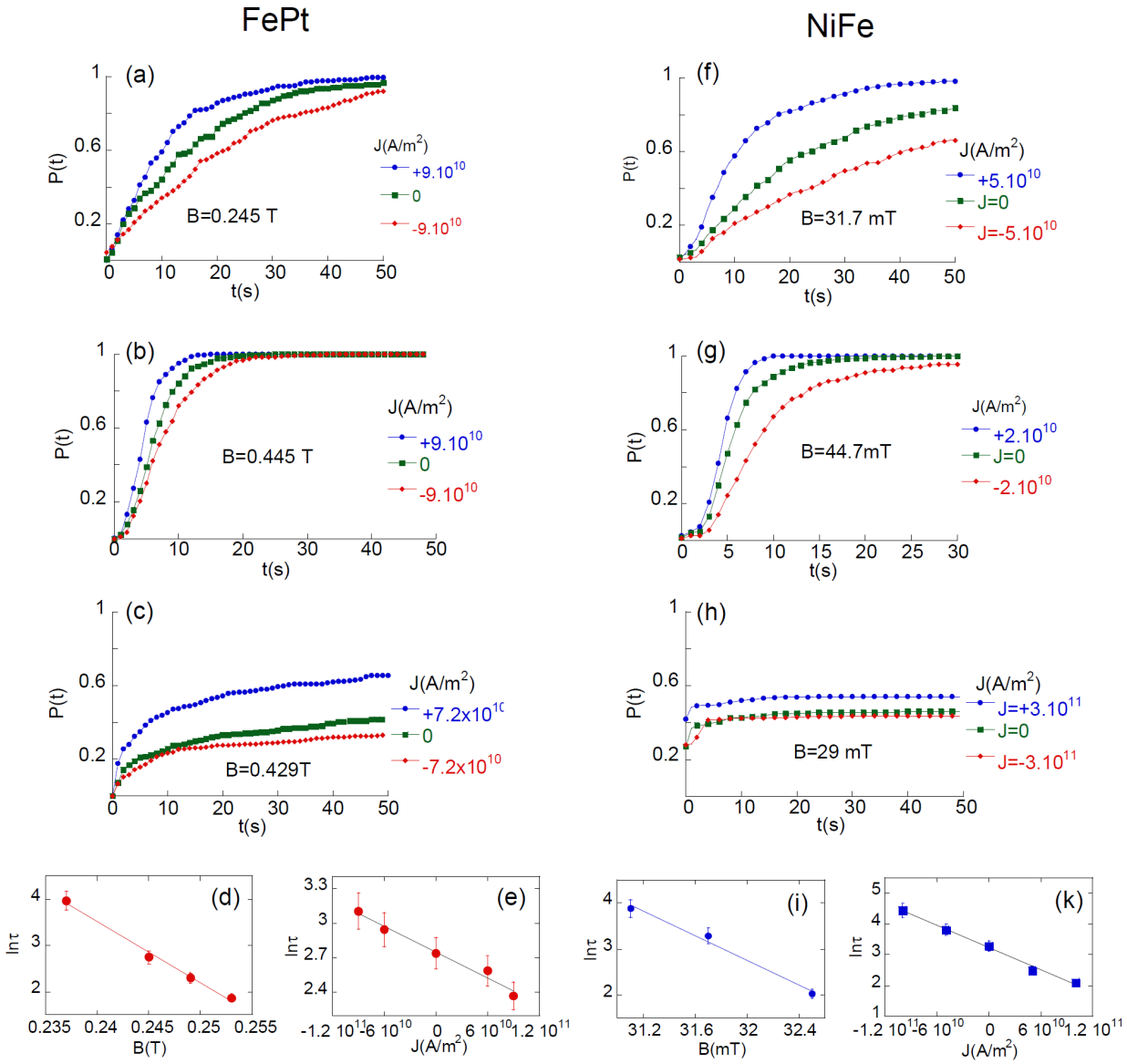


**Figure 4** | **Cumulative probability functions P(t) of depinning at constant magnetic fields, for various DC currents.** These curves show the bipolar effect due to the spin transfer torque on the depinning probability. In both FePt and NiFe systems the current-field equivalence can be generalized for the three kind of depinning processes, (a, f): simple path, (b, g): serial paths, (c, h): alternative paths. Figs. (d, e) and (i, k) shows the characteristic pinning time in the case of the simple path behavior, as a function of the applied field (d) and the applied currents (e) for FePt and (i,k) NiFe. The symbols represent experimental results and the solid lines illustrate a linear fit on a log scale.

Supplemental Material at [SM URL] for details on how to deal with these cases).

In fact, it is still difficult to predict which kind of constriction is responsible for such depinning behaviors in both systems. For FePt, this might suggests that the structural defect still affect on DW depinning process, having the same microscopic influence. The constriction acts as a filter that select one particular defect controlling the propagation. For NiFe, this might be due to the much large size of the DW that can be less controlled by structural defects.

The statistical analysis of pinning times can provide a way to measure the spin-torque efficiency[2,9,16,20]. Here, we show in fig. 4 that in both systems the current-field equivalence[29] can be generalized for the three kinds of depinning processes. In our definition, the positive current corresponds to assist DW depinning while negative current hinders DW depinning. In all measurements, the DW moves along the direction of electron flow due to the spin transfer torque effect.

Even though recent experiments[5] show that the potential landscape for current and field-induced depinning are different, here the overall behaviour is not modified when applying a current.

The data obtained for the simple path show that $\ln(\tau)$ varies linearly with both the field and the applied current (cf. figs. 4d,i,e,k). In the studied range of currents, there is no additional quadratic dependence of E with the current as those seen in ref. [4]. The efficiency of the spin transfer can thus be measured in materials possessing very different coercivities. The obtained values are $\xi_{FePt} = 4 \times 10^{-13}$ T.m$^2$/A, in agreement with previous values measured in FePt[2,16], and $\xi_{NiFe} = 1 \times 10^{-14}$ T.m$^2$/A, which is one order magnitude higher than what is observed in ref. [30].

To conclude, although we used very narrow constrictions, the landscape potential appears to be very complex, often involving several energy barriers. For wire dimensions where microscopy techniques become ineffective, and as the importance of intrinsic defects complicates the use of micromagnetic simulations, it is yet difficult to predict which kind of constriction should lead to which depinning behaviour. Moreover, the relationship between the constriction geometry and the depinning process appears to be non-trivial: in several cases, we obtained different behaviours for constrictions supposed to be completely similar. However, in both planar and perpendicular systems, the basic elements of any depinning mechanism have been observed and identified, and are found to react identically to variations of field or to the addition of a DC current. The statistical study of the depinning thus allows obtaining detailed information about the potential landscape seen by the DW.


1. Attané, J. P. *et al.* Thermally activated depinning of a narrow domain wall from a single defect. *Phys. Rev. Lett.* **96**, 147204 (2006).
2. Burrowes, C. *et al.* Non adiabatic spin-torques in narrow magnetic domain walls. *Nat. Phys.* **6**, 17 (2009).
3. Laribi, S. *et al.* Reversible and irreversible current induced domain wall motion in CoFeB based spin valves stripes. *Appl. Phys. Lett.* **90**, 232505 (2007).
4. Kim, K.-J. *et al.* Electric current effect on the energy barrier of magnetic domain wall depinning: Origin of the quadratic contribution. *Phys. Rev. Lett.* **107**, 217205 (2011).
5. Kim, K. J. *et al.* Two-barrier stability that allows low-power operation in current-induced domain-wall motion. *Nat. Commun.* **4**, 2011 (2013).
6. Fukami, S., Yamanouchi, M., Ikeda, S. & Ohno, H. Depinning probability of a magnetic domain wall in nanowires by spin-polarized currents. *Nat. Commun.* **4**, 2293 (2013).
7. Himeno, A., Kasai, S. & Ono, T. Depinning fields of a magnetic domain wall from asymmetric notches. *J. Appl. Phys.* **99**, 08G304 (2006).
8. Akerman, J., Muñoz, M., Maicas, M. & Prieto, J. L. Stochastic nature of the domain wall depinning in permalloy magnetic nanowires. *Phys. Rev. B* **82**, 064426 (2010).
9. Eltschka, M. *et al.* Nonadiabatic spin torque investigated using thermally activated magnetic domain wall dynamics. *Phys. Rev. Lett.* **105**, 056601 (2010).
10. Cucchiara, J. *et al.* Telegraph noise due to domain wall motion driven by spin current in perpendicular magnetized nanopillars. *Appl. Phys. Lett.* **94**, 102503 (2009).
11. Im, M.-Y., Bocklage, L., Fisher, P. & Meier, G. Direct observation of stochastic domain-wall depinning in magnetic nanowires. *Phys. Rev. Lett.* **102**, 147204 (2009).
12. Meier, G. *et al.* Direct imaging of stochastic domain-wall motion driven by nanosecond current pulses. *Phys. Rev. Lett.* **98**, 187202 (2007).
13. Möhrke, P. *et al.* Single shot Kerr magnetometer for observing real-time domain wall motion in permalloy nanowires. *J. Phys. D: Appl. Phys* **41**, 164009 (2008).
14. Briones, J. *et al.* Stochastic and complex depinning dynamics of magnetic domain walls. *Phys. Rev. B* **83**, 060401(R) (2011).
15. Fukami, S. *et al.* Distribution of critical current density for magnetic domain wall motion. *J. Appl. Phys.* **115**, 17D508 (2014).
16. Mihai, A. P. *et al.* Magnetization reversal dominated by domain wall pinning in FePt based spin valves. *Appl. Phys. Lett.* **94**, 122509 (2009).
17. Nguyen, V. D. *et al.* Magnon magnetoresistance of NiFe nanowires: Size dependence and domain wall detection. *Appl. Phys. Lett.* **99**, 262504 (2011).
18. Garcia-Sanchez, F. *et al.* Effect of crystalline defects on domain wall motion under field and current in nanowires with perpendicular magnetization. *Phys. Rev. B* **81**, 134408 (2010).
19. Martinez, E. *et al.* Thermal effects on domain wall depinning from a single notch. *Phys. Rev. Lett.* **98**, 267202 (2007).
20. Mihai, A. P. *et al.* Stochastic domain-wall depinning under current in FePt spin valves and single layers. *Phys. Rev. B* **84**, 014411 (2011).
21. Kim, K.-J. *et al.* Interdimensional universality of dynamic interfaces. *Nature* **458**, 740–742 (2009).
22. Laufenberg, M. *et al.* Observation of thermally activated domain wall transformations. *Appl. Phys. Lett* **88**, 052507 (2006).
23. Bogart, L. K. *et al.* Dependence of domain wall pinning potential landscapes on domain wall chirality and pinning site geometry in planar nanowires. *Phys. Rev. B* **79**, 054414 (2009).
24. Petit, D. *et al.* Domain wall pinning and potential landscapes created by constrictions and protrusions in ferromagnetic nanowires. *J. Appl. Phys.* **103**, 114307 (2008).
25. He, K., Smith, D. & McCartney, M. R. Observation of asymmetrical pinning of domain walls in notched Permalloy nanowires using electron holography. *Appl. Phys. Lett.* **95**, 182507 (2009).
26. Hayashi, M. *et al.* Dependence of current and field driven depinning of domain walls on their structure and chirality in Permalloy nanowires. *Phys. Rev. Lett.* **97**, 207205 (2006).
27. Hayward, J. *et al.* Exquisitely balanced thermal sensitivity of the stochastic switching process in macroscopic ferromagnetic ring elements. *Phys. Rev. B* **72**, 184430 (2005).
28. Klaui, M. *et al.* Controlled and reproducible domain wall displacement by current pulses injected into ferromagnetic ring structures. *Phys. Rev. Lett.* **94**, 106601 (2005).
29. Heinen, J. *et al.* Determination of the spin torque non-adiabaticity in perpendicularly magnetized nanowires. *J. Phys.: Condens. Matter* **24**, 024220 (2012).
30. Beyersdorff, B. *et al.* Thermal effects in spin-torque assisted domain wall depinning. *Phys. Rev. B* **86**, 184427 (2012).


## Acknowledgments

We acknowledge financial support from the Fondation Nanosciences (RTRA) in Grenoble and Agence National de la Recherche (ANR). The devices were fabricated at the Plateforme de Technologie Amont in Grenoble.

## Author contributions

L.V., J.P.A. and A.M. supervised the study. V.D.N. performed the experimental works, analysed results with assistance from W.S.T., M.J., C.B., L.N., L.V., J.P.A., V.D.N. and A.M. wrote the manuscript. All authors discussed the results.

## Additional information

**Supplementary information** accompanies this paper at http://www.nature.com/scientificreports

**Competing financial interests:** The authors declare no competing financial interests.

**How to cite this article:** Nguyen, V.D. *et al.* Elementary depinning processes of magnetic domain walls under fields and currents. *Sci. Rep.* **4**, 6509; DOI:10.1038/srep06509 (2014).